Journal of Applied Polymer Science

Spectroscopic Analysis and Catalytic Application of Biopolymer Capped Silver Nanoparticle, an Effective Antimicrobial Agent

Nilkamal Pramanik, Aditi Bhattacharyya, Patit Paban Kundu
Advanced Polymer Laboratory, Department of Polymer Science and Technology, University of Calcutta, Kolkata, West Bengal 700009, India
Correspondence to: P. P. Kundu (E-mail: ppk923@yahoo.com)

ABSTRACT: Microbial reduction of silver ion (conc. 1 m*M* $AgNO_3$) was performed by *Alkaliphilus oremlandii* strain ohILAs in an alkaline pH 10. The synthesized silver nanoparticle was stabilized by poly(3-hydroxybutyrate-*co*-3-hydroxyvalerate) biopolymer which was also synthesized by the microbial culture of *Alkaliphilus oremlandii* strain ohILAs at pH8. The particle size and shape of the silver nanoparticles was studied by dynamic light scattering and under a transmission electron microscope and it was found that the particle size of polymer stabilized colloidal silver was comparatively lower (22–43nm) than that for the unstabilized one (63–93 nm). The stabilization of nanoparticles in polymer dispersed medium after around 60 days was confirmed from analysis of UV-visible spectroscopy and scanning electron microscopy. The crystalline peaks as recorded with X-ray's diffraction were observed at 2θ values of 38° and 43°, indicating the fcc crystalline structure of the silver nanoparticle. The antimicrobial activity of silver nanoparticles on gram-negative bacteria strain (*Escherichia coli* XL1B) and gram-positive strain (*Lysinibacillus fusiformis*) showed better performance by the solution of polymer stabilized nanoparticle than that for the non polymer stabilized one. The reduction of nitro group in *p*-nitrophenol to *p*-aminophenol was observed from the analysis of UV-Visible spectroscopy in which, the shifting of absorption peak at 400 to 295 nm and the simultaneous regeneration of light brown color (λ_{max} 410 nm) of silver nanoparticles confirmed the catalytic activity of silver nanomaterials. © 2014 Wiley Periodicals, Inc. J. Appl. Polym. Sci. **2015**, *132*, 41495.

KEYWORDS: biosynthesis of polymers; nanoparticles; nanowires and nanocrystals; spectroscopy

Received 25 March 2014; accepted 4 September 2014
DOI: 10.1002/app.41495

INTRODUCTION

Nanoparticle is the most essential tool for modern technology due to its use in many devices such as semiconductor, photonics, and other diverse fields.[1,2] In biomedical fields, different types of applications such as drug delivery, nucleic acid delivery and cell apoptosis through nanocarrier show unique and versatile application of nanotechnology.[3,4] The random uses of nanoparticles are due to their specific properties such as size, antimicrobial activity, nontoxicity, and especially higher surface to volume ratio. Different types of metal nanoparticles such as copper, gold, palladium, rhodium, platinum, silver, iron, and so forth have been developed for the biomedical application and also for catalytic activity in synthetic chemistry. Catalysts play an important role not only in industrial chemical processes but also in enzymatic reactions in the human body. Colloidal dispersed metal nanoparticles are nearly similar in function as enzyme, thus, sometimes it is called artificial enzyme[5]; but polymer capped metal nanoparticles are more preferred ones than colloidal dispersed nanoparticles due to its high selectivity and shielding effect, causing retainment of its activity as catalyst for longer duration. Many chemists have synthesized metal nanoparticles by using different chemical procedures and used them as catalysts in different reaction mechanisms.[6] The use of Iridium (Ir°), Rhodium (Rh°) nanoparticles as catalysts were reported for the homogeneous or heterogeneous hydrogenation of arenes in the selective organic synthesis.[7] In Heck reaction,[8] the coupling of styrene and 4-bromoacetophenone was successfully performed by using palladium nanoparticles stabilized by polystyrene-*b*-poly-4-vinylpyridine. The formation of ring structure via cycloaddition of alkynes with alkenes and carbon monoxide to cyclopentenones (Pauson-Khand reaction[9]) was also reported by using chemically synthesized Cobalt nanoparticles. The cross-coupling reactions of aryl halides with arylboronic acids in the presence of Palladium nanoparticle, often referred as Suzuki coupling reactions, is a versatile method for the synthesis of unsymmetrical biaryls compound.[10]

Additional Supporting Information may be found in the online version of this article.

The hydrophobic fields that surround metal nanoparticles can play another important role to improve the catalytic activity[11] of nanoparticles. The micelles surrounding metal nanoparticles are one of the most interesting examples. The hydrophobic field can accelerate the charge separation and provide an aligned field, suitable in photochemical hydrogen generation (artificial photosynthesis) by the favorite interactions with cation radicals of viologen rather than those with dications[12] and for region-selectivity in the catalytic reactions.[11] But, these nanoparticles are not useful for biomedical applications like the treatment from burns to prevent infections as well as in dental-surgery and in vascular grafts due to its toxic nature.[13–16] Due to this major problem, researchers are trying to replace the environmental toxic precursors via ecofriendly synthesis of lower ranges (10–50 nm) metal nanoparticles. Among different types of nanoparticles, silver nanoparticle can be used as a cheap ingredient in products such as detergents, cosmetics, sun-screen lotions and also in medicine[17] Krishnaraj et al. already synthesized silver nanoparticles of 20–30 nm size through benign and green pathways. Microorganisms, fungus, yeasts are found to reduce the silver ion to nanosilver via enzymatic pathways within their cellular core.[18,19] Silver resistant bacteria such as *Pseudomonas stutzeri* AG259 is also capable to accumulate silver nanoparticles through the intracellular reduction of the silver monopositive ion.[20] The bacterial synthesis of lower sized silver nanoparticles is more attractive due to their low cost of production and also for their antimicrobial, anti fungal and antiviral activity.[21–23] The efficient antimicrobial activity of microbially synthesized silver nanoparticles is the key component for their use in biomedical applications. Silver nanoparticles with their antifungal and antiviral activity are also a major contribution in the field of nanomedicine. Kim et al. and Elechinguera et al. experimentally proved the antifungal and antiviral activity of silver nanoparticles.[24,25] A large volume of silver nanoparticles is synthesized by the consecutive microbial reduction of silver monopositive ion. In this method, low concentrated microbial cells are enough to convert large volume of silver ion to silver nanosol, whereas another chemical reducing agent could be an expensive as well as toxic proponent for the environment and the living cell. Both extracellular and intracellular pathways are utilized for the synthesis of silver nanoparticles.[19,20] But, the extracellular synthesis of silver nanoparticles shows an added advantage over intracellular production for their easy separation. The extracellular pathways also serve as an electron shuttle for the metal ion reduction by the reductase (released from microorganisms) to the nanoparticles. Therefore, to overcome the chemical toxicity and intracellular hazards, extracellular synthesis provides a feasible alternative. But, the long-time stability of colloidal nanoparticles is an important aspect. A number of authors were able to find a way out for successful colloidal stability of silver nanoparticles by using hydrophobic polymer and capping agent.[26] The limited use of the nanoparticle in more optimized applications is due to its toxicity and aggregation in solution. Therefore, these problems can be solved by the use of a hydrophobic biopolymer, Poly (3-hydroxybutyrate-*co*-3-hydroxyvalerate) as a stabilizing agent which would prevent the agglomeration of silver nanoparticle from the colloidal solution. At this point of view, short-time microbial synthesis of silver nanoparticle with smaller size of particle and maintaining its long time stability for the usage as catalysts are the artworks of this research work. In this work, we have used *p*-nitrophenol as a model compound which is water soluble and is easily available to investigate the catalytic function of polymer capped silver nanoparticles. The use of the model compound, *p*-nitrophenol has been reported by a number of researchers to examine the catalytic efficiency of prepared metal nanoparticles.[27,28]

EXPERIMENTAL

Materials

Chloroform, methanol, and nutrient broth were purchased from MERCK India. Silver nitrate solution, para-nitrophenol, sodium borohydride were also purchased from MERCK India to carry out the research work.

Isolation of *Alkaliphilus oremlandii* OhILAs Strain

The rhizosphere soil was collected from the University of Calcutta campus and *Alkaliphilus oremlandii* OhILAs *sp.* was isolated by using serial dilution method. The specific media used for the isolation of *Alkaliphilus oremlandii* strain ohILAs was composed of NH_4NO_3 (0.3 g), K_2HPO_4 (1.0 g), $MgSO_4.7H_2O$ (0.2 g), $FeSO_4.7H_2O$ (0.05 g), $CaCl_2.2H_2O$ (0.1 g), $Na_2MoO_4.2H_2O$ (1 mg), glucose (10 g) per liter basis; pH of the media was maintained at 8.0 and the isolation was done at 30°C.

Microbial Synthesis of Polyhydroxyalkanoates

Alkaliphilus oremlandii strain ohILAs was inoculated in nitrogen limited growth medium. The medium consists of 0.3 g NH_4NO_3, 0.064 g K_2HPO_4, 0.02 g KH_2PO_4, 0.04 g $MgSO_4.7H_2O$, 0.01 g $CaCl_2.2H_2O$, 1 mg $FeS0_4.7H_2O$, 0.6 mg $Na_2MoO_4.2H_2O$, 0.05 g Na-Citrate in 100 mL distilled water. Waste cooked rapeseed oil (2%) was used as carbon source. Different initial pH of the medium (5 to 10) was used to check whether the pH has any effect on Polyhydroxybutyrate (PHB) production. Then, it was sterilized in an autoclave at a pressure of 15 psi and at 121°C temperature for 15 min. Cells were grown in an orbital shaker (105 rpm) at a temperature of range 25–40°C and harvested after 72, 84, and 96 h of incubation respectively by the centrifugation at 6000 rpm for 10 min. Finally, the cell pellet was resuspended and washed twice with saline water before cell disruption in Na-hypochlorite solution.

Extraction of PHA

Hypochlorite-Method. The copolymer was extracted from the bacterial cell using chloroform-hypochlorite method.[29] After 72, 84 and 96 h of incubation at a temperature of 25–40°C and pH of 5 to 10, 10 mL of each microbial culture was centrifuged for 10 min at 6000 rpm. The pellet was collected and washed with 10 mL of saline solution and recentrifuged in the same way. Then, the pellet was suspended in 5 mL of sodium hypochlorite (4% active chlorine) and digested at 37°C for 40 min with stirring, followed by extraction with hot chloroform and precipitated with methanol. The extracted polymers were recentrifuged and washed with 10 mL of cold diethyl ether to get purified P(3HB-*co*-3HV). The procedure for PHA extraction and purification was the similar one as described in the previous report.[30]

The polymers were then vacuum-dried for 48 h. The polymer yield was determined using the following formula:

$$S = \frac{P}{W} \times 100 \quad (1)$$

S represents the polymer yield (weight %), P is the polymer weight (g) and W is the dried cell mass (g).

Cell Dry Weight. After centrifugation of the culture medium, the supernatant was discarded and the cell pellet was washed with double distilled water. The washed pellet was then resuspended in 1 mL of double distilled water for proper washing and then dried to constant weight at 60°C. The dry weight of the cells was determined by drying the washed cells to constant dry weight (W).

Microbial Culture for Biomass Production. The *Alkaliphilus oremlandii* strain ohILAs was cultured in a nutrient broth medium. The broth medium was sterilized and inoculated at 30°C in an orbital shaker (120 rpm) for 36 h. Then, 10 mL of microbial culture was centrifuged for 10 min at 6000 rpm. The pellet and supernatant were separately collected for microbial synthesis of silver nanoparticles according to the method reported by Das et al.[31]

Reduction of Silver Nitrate Solution to Metallic Silver. The synthesis of metallic silver nanoparticles was carried out by using *Alkaliphilus oremlandii* strain ohILAs in the presence and absence of polyhydroxyalkanoates dispersed medium. The polymer dispersed medium was prepared by using a water bath homogenizer. The supernatant of bacterial culture was used for the production of silver nanoparticles where 50 mL of supernatant of bacterial culture was mixed with 50 mL of sterilized polymer dispersed aqueous $AgNO_3$ solution (1 mM). At the same time, 2 g of wet bacterial biomass was resuspended in 100 mL aqueous solution of polymer dispersed medium containing 1 mM of $AgNO_3$ in a 250-mL Erlenmeyer flask. In addition, two different sets of reaction mediums were used in the absence of stabilizer to carry out the microbial reduction of silver monopositive ion (Ag+) by using the pellet and the supernatant of culture. The microbial reduction of silver ion was performed in the pH range of 5 to 10 and all the reaction mixtures were incubated on a rotating shaker (105 rpm) under bright condition for 24 h. The experimental condition is in agreement with the method described by Natarajan et al.[32]

Antimicrobial Studies. The AgNPs synthesized from *Alkaliphilus oremlandii* strain ohILAs were tested for antimicrobial activity by disk diffusion method[33] against *Escherichia coli* XL1B strain (gram-negative), *Lysinibacillus fusiformis* strain (gram-positive). The inhibitory effect was tested on a sterilized agar plate of liquid nutrient broth which contains animal tissue (5.0 g/L), NaCl (5 g/L), beef extract (1.5 g/L) and yeast extract (1.5 g/L). The broth was solidified by using 1.3 g/L of agar. Approximately 10^5 colony-forming units of each strain (gram positive and gram negative bacterial strain) was swabbed uniformly on an agar plate using sterile cotton swabs to incubate at 37°C. Different concentrated solutions (30, 40, 50, and 60 μg/cm^3) of silver nanoparticles were then poured onto each of four selected zones of the agar plate and kept for 24 h to observe the bactericidal effect on those microorganisms at 37°C.

Catalytic Reduction of Para-Nitrophenol. Functional group conversion of the nitrogroup in para-nitrophenol to para-aminophenol was observed in the presence of polymer stabilized silver nanoparticle and ice cold sodium borohydride in a standard quartz cuvette with a 1-cm path length. About 1 mL of silver sol and 100 μL of the nitro compound (aqueous solution; 1.2×10^{-3} M) were taken. Then, 60 μL aqueous ice cold solution of $NaBH_4$ (0.1M) was added to the mixture. Then, the formations of the product with the gradual discoloration of yellow solution were observed through UV-visible spectrophotometry (optizen view, made of Mecasys, Korea) in the range of 200–800 nm at 25°C. After the yellow color was completely discharged, the peak due to nitrocompounds was no longer observed. Conversely, the appearance of a new peak at 430 nm was noticed after 8 min of the completion of the reaction. The experimental observation is in agreement with the similar experiment reported by Gangula et al.[28]

Characterization

UV-Visible Spectra Analysis. The absorbance and reduction of Ag+ ion present in the samples taken in quartz cuvettes were monitored by using UV-Visible spectrophotometer (Optizen view, Mecasys, Korea) at a resolution of 1 nm.

Analysis of Fourier Transform Infrared Spectroscopy Spectra. Fourier transform infrared (FTIR) spectra of both biopolymer and metallic silver nanoparticle was carried out with an attenuated total reflectance (ATR)-FTIR (model-Alpha, Bruker, Germany) spectrometer, scanning from 4000 to 550 cm^{-1} for 42 consecutive scans at room temperature. The stretching frequency of each functional groups (C—H, C—C, C—O, C═O) was recorded. Polyhydroxyalkanoates (1 mg) was mixed with 25 mg of KBr to form KBr pellet for the IR analysis at 27°C. The pellet of Ag nanoparticles obtained after centrifugation, was redispersed with distilled water and finally FTIR-ATR measurement was performed.

X-ray Diffraction Study. X-ray diffraction (XRD) measurement was recorded at 40 kV, 30 mA on a Rigaku (RAD-111B) diffractometer using nickel filtered CuK_α radiation (wave length of 0.154 nm). The X-ray analysis was studied at 27°C in the temperature range of 5–50°C at a scanning speed of 20/min.

Particle Size Measurement. Particle size of synthesized silver nanoparticles was analyzed by using a laser particle size analyzer (Malvern, Zetasizer Nano series, nano ZS90). The diameter of nanoparticle was measured through dynamic light scattering (DLS) measurement.

Scanning Electron Microscopy Analysis. The morphological examination of the synthesized silver nanoparticles was carried out using a scanning electron microscope (SEM; Model: Philips XL30, Carl Zeiss, Germany) after coating the sample with gold under vacuum.

Transmission Electron Microscopy Analysis. Size and shape of the silver nanoparticle was analyzed from the micrograph of the transmission electron microscopy (TEM) which was performed

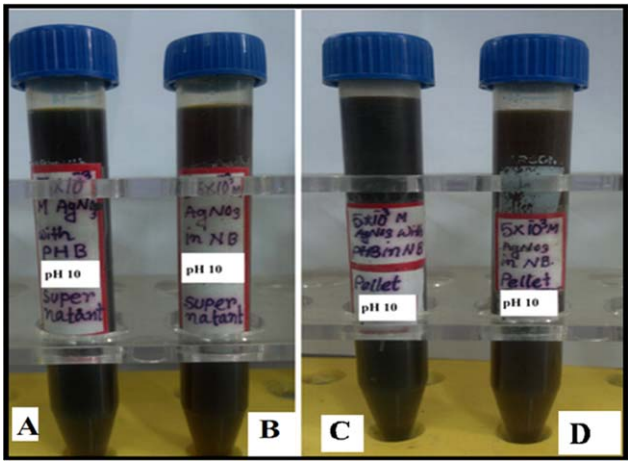

Figure 1. Microbial reduction of silver nitrate solution in (A) polymer stabilized and (B) unstabilized supernatant portion of bacterial culture, (C) polymer stabilized and (D) unstabilized pellet portion of bacterial culture. [Color figure can be viewed in the online issue, which is available at wileyonlinelibrary.com.]

on a JEOL JEM 2100 HR. The grid for TEM analysis was prepared by placing a drop of the nanoparticle suspension on a carbon-coated copper grid and allowing the water to evaporate inside a vacuum dryer. The grid containing silver nanoparticles was scanned by a TEM.

Statistical Analysis

The antimicrobial activities were done in triplicates and reported values were the means of triplicate counts ± standard deviations (SD).

RESULTS AND DISCUSSIONS

Identification of Isolated Strains

Isolated strain was identified using the full-length sequences using 16S rDNA technique and compared to those available in the public databases. The results showed that the isolated strain was closely related to the bacterial strain, *Alkaliphilus oremlandii* strain ohILAs and the allotted accession number for 16S rDNA sequences is (NR_043674.1).

Synthesis of Silver Nanoparticles

The bioreduction of 1 m*M* $AgNO_3$ was performed by using a microbial culture of *Alkaliphilus oremlandii* strain ohILAs and the immediate color change was monitored by the UV-Visible spectrophotometer. The appearance of a reddish brown color in the reaction vessel suggested the possible formation of Ag-NPs. The formation of reddish brown color was solely depended on the pH of the media and it was observed that the optimum value of pH for the reduction was in the range of 9–10. At low pH, the enzymatic reduction process was not suitable for the synthesis of metallic nanoparticle. On the other hand, in alkaline pH, the appearance of dark brown color indicated the formation of silver nanoparticle within 60 min of incubation period (Figure 1 and Supporting Information Figure S1). The dark brown color of microbially synthesized silver nanocrystal in polymer dispersed medium was potentially more effective than unprotected medium due to the coherent oscillation of electrons at the surface of nanoparticles resulting in surface Plasmon resonance.[34]

UV-Visible Spectral Analysis

The appearance of strong absorption peaks by placing the brown color solution under UV-Vis light was shown in Figure 2. The intense absorption peak of four sets of samples

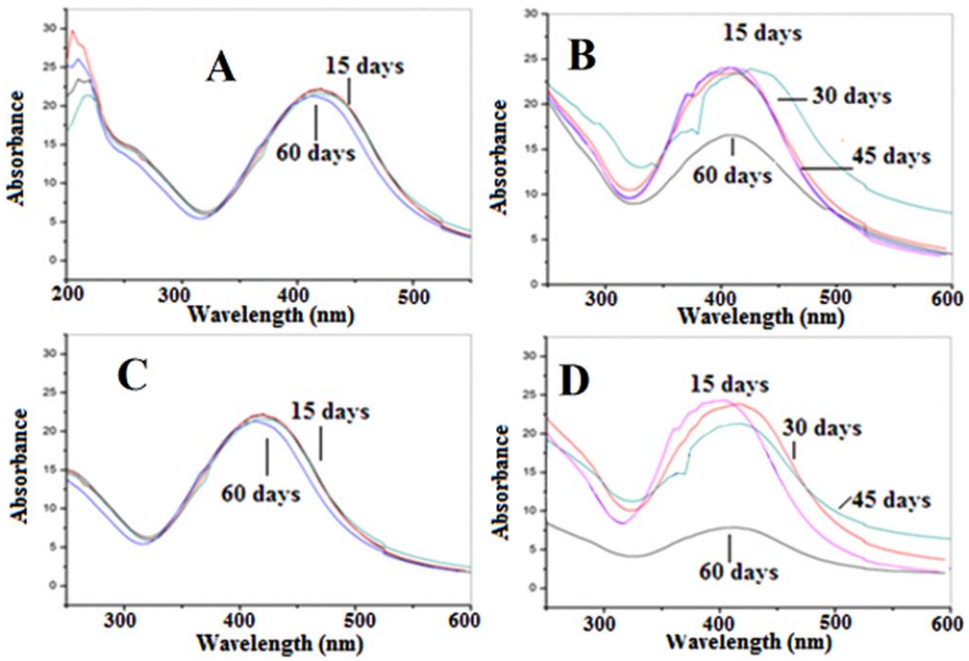

Figure 2. UV-Visible spectra of polymer stabilized supernatant portion; (A) unstabilized supernatant portion (B), polymer stabilized pellet portion (C) and unstabilized pellet portion (D) of bacterial culture after 1 day and 60 days, respectively. [Color figure can be viewed in the online issue, which is available at wileyonlinelibrary.com.]

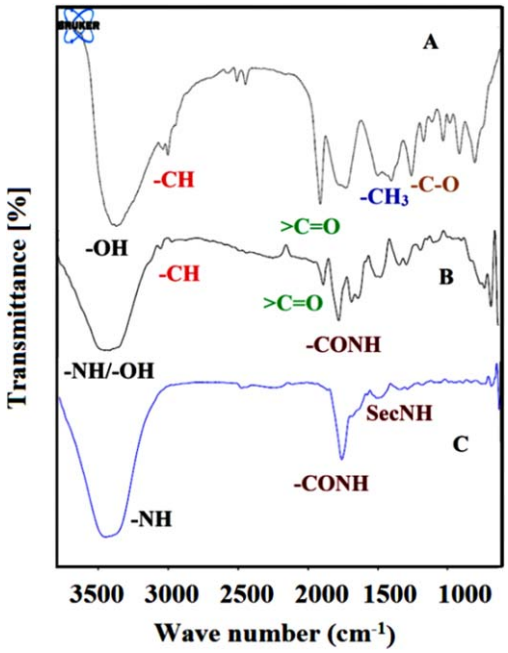

Figure 3. (A) FTIR spectra of poly(3-hydroxybutyrate-*co*−3-hydroxyvalerate) copolymer and (B) ATR spectra of Polymer stabilized silver nanoparticles and (C) unstabilized silver nanoparticles. [Color figure can be viewed in the online issue, which is available at wileyonlinelibrary.com.]

(protected/unprotected polymer of both pellet and supernatant) were observed at around 405–420nm. Observation of this strong but broad surface plasmon peak has been well documented for various Ag-NPs, with sizes ranging from 10 to 100 nm.[31] This was due to the presence of well-dispersed metallic silver nanoparticles. The absorption bands of these intense color solutions were recorded for 60 days. The stability was also traced up to 60 days at a given time interval of 15 days by the UV-visible spectroscopy. The UV-visible spectra [Figure 2(A,C)] showed that the peak intensity of polymer protected medium remains unchanged throughout the whole observation period, whereas the intensity of the plasmon absorption band displayed a slight decrease after 45 days of storage. The optical density [Figure 2(B,D)] of unprotected nanosol was found to decrease after 45 days due to the agglomeration of metallic nanoparticles. Likewise, the maximum intensity of the absorbance peak exhibited a bathochromic shift of 10 nm during this time. This may possibly be due to the ripening of the nanoparticles.[35] From these results, one can easily conclude that the silver colloidal solution was prepared by using poly(3-hydroxybutyrate-*co*-3-hydroxyvalerate) biopolymer dispersed medium at optimal conditions and was very stable against aggregation during their storage for long time (more than 60 days). Therefore, polyhydroxyalkanoates enhanced long-term stability of the microbial synthesized nanoparticle in comparison to the earlier reported results.[36]

FTIR Analysis of Polyhydroxyalkanoates and Silver Nanoparticles

Figure 3 shows the FTIR spectra of polyhydroxyalkanoates, PHAs stabilized silver nanoparticles and only silver nanoparticles. In Figure 3(A), a strong band at 1283 cm^{-1} indicates the presence of an ester bond in the copolymer. The absorption peak at 1383 cm^{-1} corresponds to the stretching of methyl (—CH_3) group, whereas the peak at 1449 cm^{-1} is due to the bending mode of vibration of methylene (—CH_2) group. In addition, the peaks at 2930, 1727 and 3429 cm^{-1} are due to the asymmetric stretching vibration of methine (—CH), carbonyl(—C═O) and hydroxyl ([sbond OH) groups, respectively. In case of polymer stabilized Ag nanoparticles [Figure 3(B)], the peaks at 1283, 1745, 3000 cm^{-1} are assigned to the stretching vibrations of ester functional groups with methyl group as a side chain. The characteristic strong resonance stretching frequencies at 1643, 1391, 1173 cm^{-1} are due to the absorption bands of silver nanoparticles. The FTIR spectrum [Figure 3(C)] of unstabilized silver nanoparticles showed that the nanoparticles manifested absorption peaks at 1654, 1562, and 1385 cm^{-1}. The appearance of these absorption peaks are due to the presence of the amide linkages of the proteins bound to the nanoparticle surface and those nanoparticles present in solution in the native form. In addition, there is a broad absorbance peak at 3225–3350 cm^{-1}. This is probably due to the presence of overtones of amide II and the terminal resonance of N—H stretching of protein excreted by a bacterial strain.[37,38] Therefore, FTIR-ATR spectra of polymer dispersed colloid solution of Ag nanoparticle confirms that the nanoparticle is capped by the polymeric network to make it a stable one.

X-rays Diffraction Analysis

The exact crystalline nature of the silver nanoparticles formed by the microbial reduction of silver nitrate solution can be achieved by measuring the XRD-spectrum of the samples and the obtained XRD pattern has been represented in Figure 4. Before the XRD characterization, the polymer stabilized silver nanoparticles and unstabilized silver nanoparticles were centrifuged at 6000 rpm for 10 min, followed by the redispersion of the pellet of silver nanoparticles into 10 mL of deionized water. After freeze drying of the purified silver particles, the

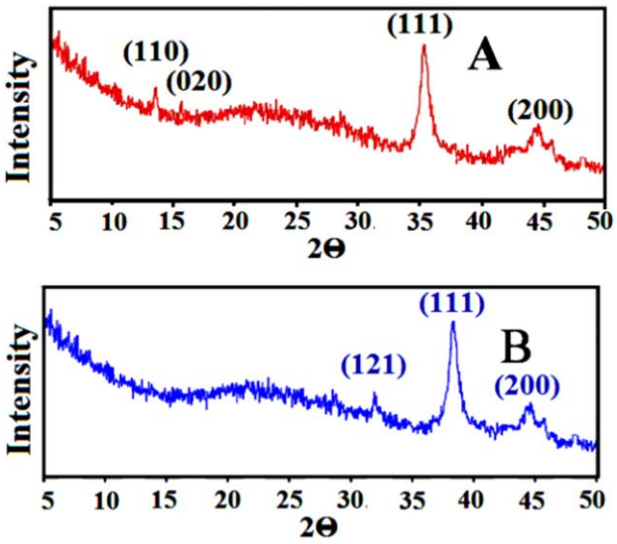

Figure 4. XRD patterns of Polymer stabilized silver nanoparticles (A), unstabilized silver nanoparticles (B). [Color figure can be viewed in the online issue, which is available at wileyonlinelibrary.com.]

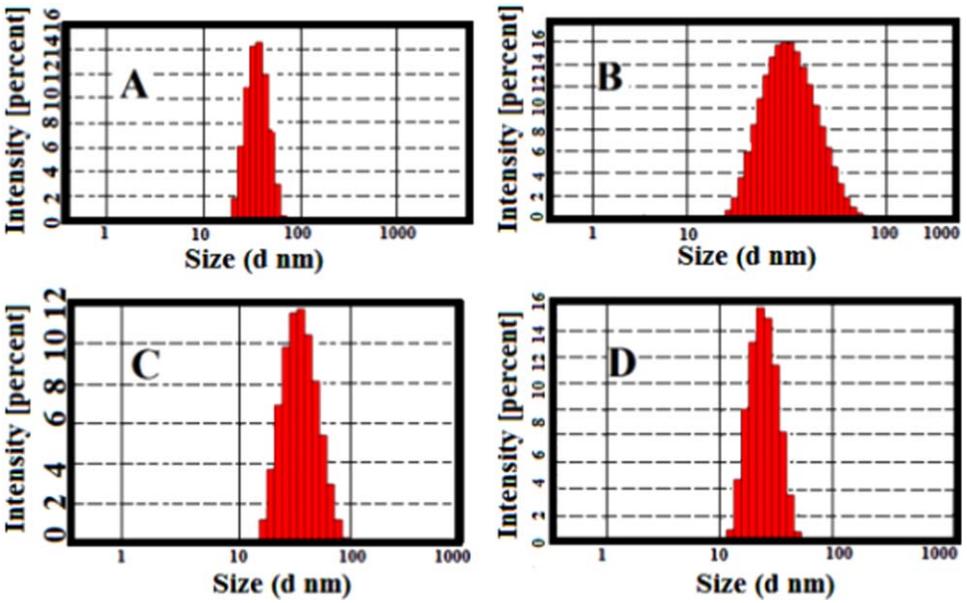

Figure 5. DLS analysis of Polymer stabilized silver nanoparticles of supernatant portion (A), and unstabilized silver nanoparticles supernatant portion (B), polymer stabilized silver nanoparticles of pellet portion (C) and unstabilized silver nanoparticles of pellet portion (D). [Color figure can be viewed in the online issue, which is available at wileyonlinelibrary.com.]

crystallinity of the silver nanoclusters in powder form were measured by XRD and the diffraction pattern of the polymer stabilized and unstabilized metal nanopowder were shown in Figure 4(A,B). The polymer stabilized nanoparticles showed three intense peaks at $2\theta = 13°$, 16.2°, 37° and 43°. Bragg's reflections at 37° and 43.3° clearly indicated the presence of (111) and (200) sets of lattice planes, revealing the presence of pure metallic nanosilver.[39] Two additional peaks at 13°, 16.2° indicated the presence of polyhydroalkanoates as cosubstance. But, such types of additional peaks were not found in unprotected silver nanoparticles. In this study, the X-ray pattern of the synthesized silver nanoparticles matched the fcc structure of the bulk silver. The remarkably intensive diffraction peak at a value of 37°from the (111) lattice plane of face-centered cubic silver unambiguously indicated that the particles were made of pure silver and that their basal plane should be the (111) plane.

The appearance of a broadened peak was probably related to the presence of various semicrystalline biopolymer capped the silver nanoparticles. The XRD results clearly showed that the silver nanoparticles formed by the reduction of Ag+ ions by the *Alkaliphilus* strain are stable over a long period of time and the nanoparticles have no tendency to agglomerate, thus indicating effective capping by the polymeric network.

DLS Analysis

The average hydrodynamic diameter (D_h) and particle size distribution (PDI) of protected and unprotected silver nanoparticles were measured by DLS. The particle size of polyhydroxyalkanoates stabilized silver nanoparticles was found to be very much smaller [Figure 5(A,D)] than unprotected nanoparticles as shown in Figure 5(B,C). Again, the average diameter of nanoparticles obtained from the incubation of microbial pellet and supernatant were found to be different to some extent. The particle size of well-dispersed polymer stabilized nanoparticles was in the ranges of 22 (±2) nm and 42 (±3) nm with a PDI of 0.303 (±0.032) and 0.492 (±0.021) for both pellet and supernatant mediated mediums, respectively. But, in case of unstabilized nanoparticles, the particle size [average hydrodynamic diameter (D_h)] were 63 (±3) nm, 92 (±2) nm, and the values of PDI were 0.537 (±0.042) and 0.356 (±0.011) for both pellet and supernatant mediated mediums, respectively (see Table I).

Scanning Electron Microscopic Analysis

The shape and morphologies of silver nanoparticles were characterized by scanning electron microscopic analysis. The function of the stabilizer was identified by comparing the

Table I. Changes of Average Hydrodynamic Radius and PDI of Ag Nanoparticles for Both Polymer Stable and Unstable Medium

Sample	Average hydrodynamic radius (nm)	Polydispersity index (PDI)
Polymer dispersed pellet mediated colloidal solution of silver nanoparticles	22.85	0.303
Pellet mediated colloidal solution of silver nanoparticles	93	0.356
Polymer dispersed supernatant mediated colloidal solution of silver nanoparticles	42.66	0.492
supernatant mediated colloidal solution of silver nanoparticles	63.58	0.537

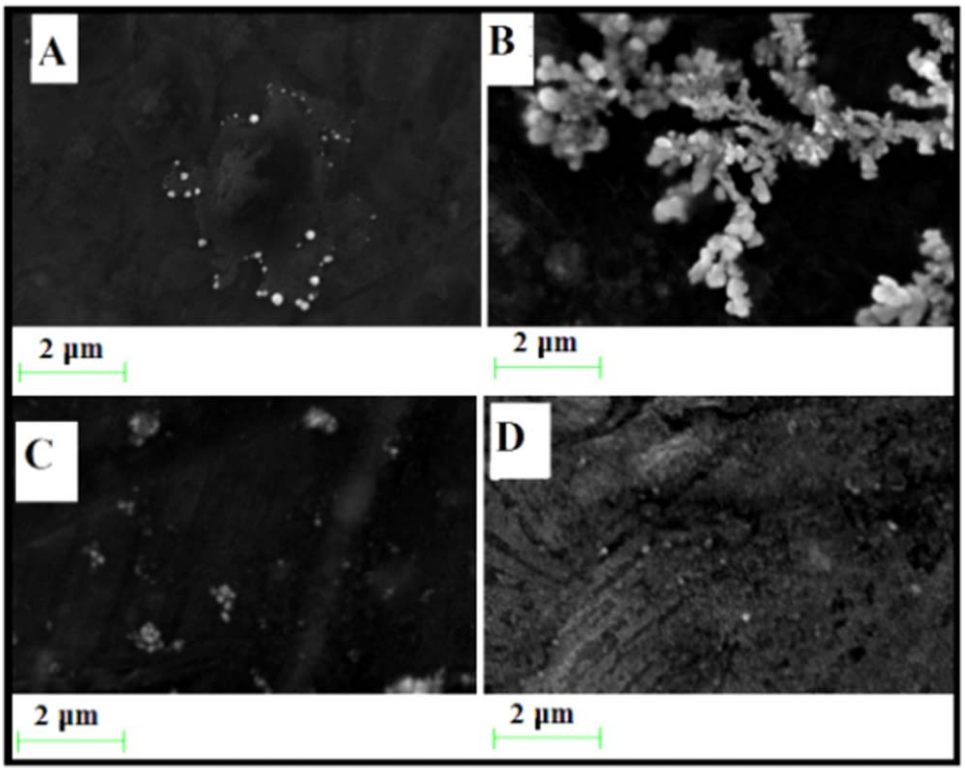

Figure 6. SEM images of polymer stabilized silver nanoparticles of pellet portion (A), unstabilized silver nanoparticles of pellet portion (B), polymer stabilized silver nanoparticles of supernatant portion (C) and unstabilized silver nanoparticles of supernatant portion (D). [Color figure can be viewed in the online issue, which is available at wileyonlinelibrary.com.]

SEM images as shown in Figure 6. The SEM micrographs [Figure 6(A,C)] of protected nanoparticles obtained in the filtrate showed that AgNPs were of spherical shape, well distributed without any aggregation in the solution. The morphology of silver nanoparticles was in agreement with the shape of the surface plasmon resonance band in the UV-Visible spectra.[40] The surface of silver nanoparticles in polymer dispersed medium was remained protected by polymeric screen as long as the observation periods hovered around 60 days. The unprotected particles were found to aggregate [Figure 6(B,D)] because the attractive force between nanoparticles was dominated over the repulsive force, whereas at the stabilizing condition, predominant repulsive force between nanoparticles prevented them to aggregate and remained active in solution.[41]

Transmission Electron Microscopic Analysis

TEM micrograph of the prepared colloidal solution of silver nanoparticles was shown in Figure 7. The micrograph showed nanoparticles with variable shape, most of them present as sphere and some others having occasional triangular shape. The rod shaped morphology of silver nanoparticles appeared to be reasonably monodispersed and the size distribution of stabilized silver nanoparticles was narrow as shown in Figure 7(A,C), having an average diameter of 18 nm. Majority of the silver nanoparticles were scattered with only a few of them showing aggregates of varying sizes as observed under TEM. This TEM image suggests that there is no tendency of clustering of nanoparticles as they are well separated from each other. The nanoparticles are not in direct contact even within the aggregates, indicating stabilization of the nanoparticles by a capping agent, polyhydroxyalkanoates. The separation between the silver nanoparticles as observed from the TEM images may be due to

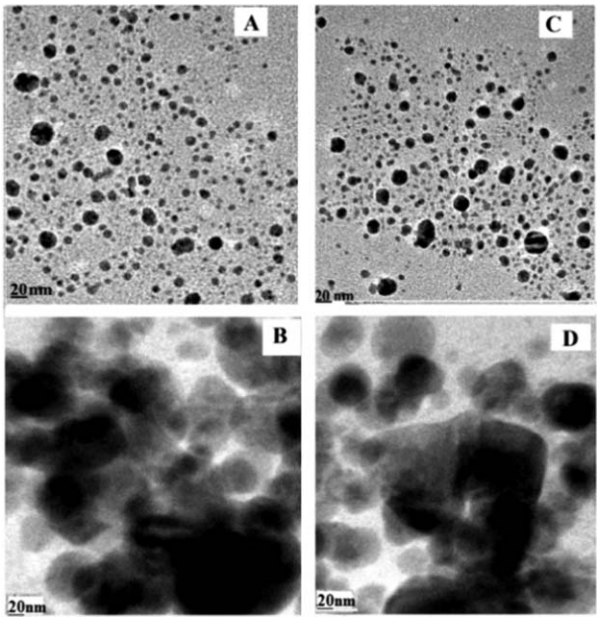

Figure 7. TEM images of Polymer stabilized silver nanoparticles of pellet portion (A), unstabilized silver nanoparticles of pellet portion (B), polymer stabilized silver nanoparticles of supernatant portion (C) and unstabilized silver nanoparticles of supernatant portion (D).

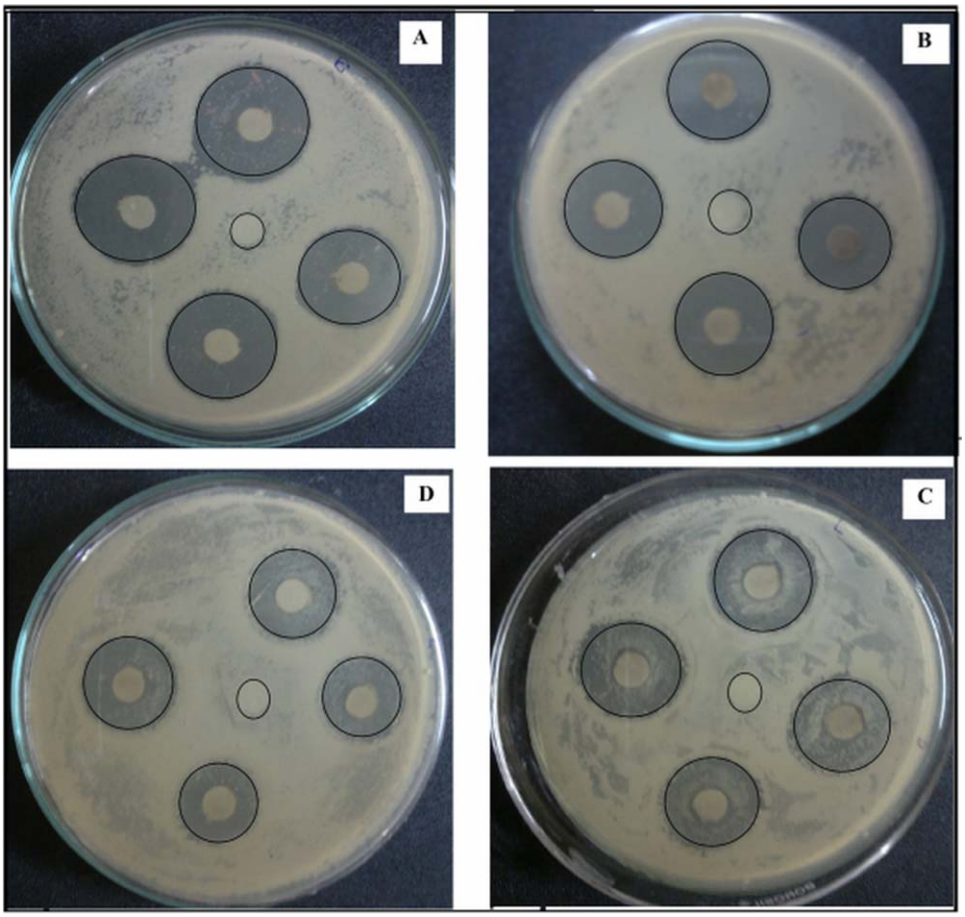

Figure 8. Zone inhibition [(mean ± SD) mm] of polymer stabilized silver nanoparticles (A) and unstabilized silver nanoparticles against *E.coli* XL1B and *Lysinibacillus fusiformis*. [Color figure can be viewed in the online issue, which is available at wileyonlinelibrary.com.]

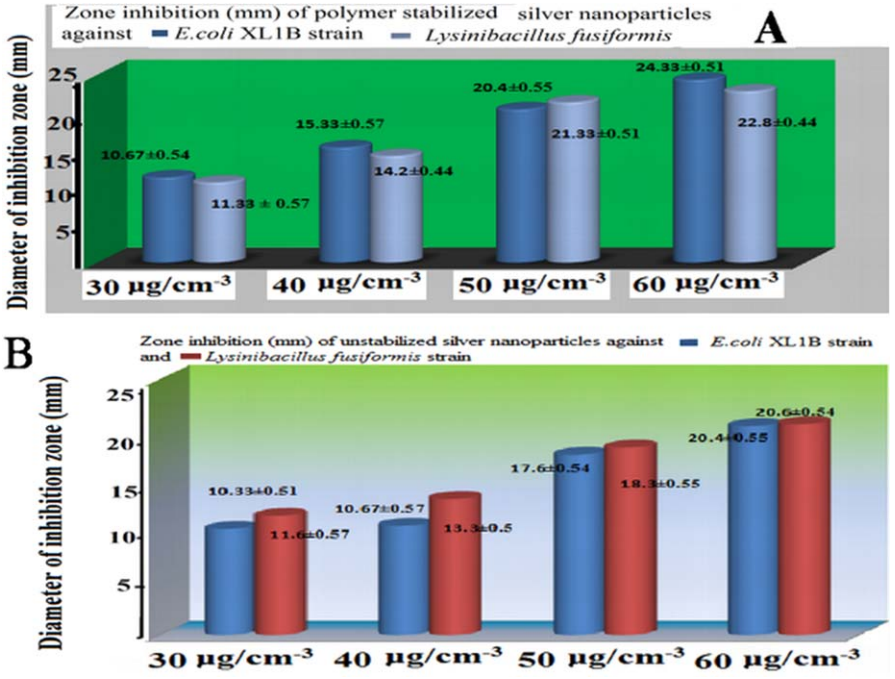

Figure 9. Images of antibacterial activities of polymer stabilized/nonstabilized silver nanoparticles against *Lysinibacillus fusiformis* strain (gram-positive) (B and D), *Escherichia coli* XL1B strain (gram-negative) (A and C). [Color figure can be viewed in the online issue, which is available at wileyonlinelibrary.com.]

Table II. Zone of Inhibition (mm) and Minimum Bactericidal Concentration of Silver Nanoparticles Against *E.coli* XL1B and *Lysinibacilus fusiformis* Bacteria

Microorganisms	Mean diameter of inhibition zone [(Mean±SD)mm] against various concentrations of Polymer stabilized Silver nanoparticles (μg/cm^3)				Mean diameter of inhibition zone [(Mean±SD) mm] against various concentrations of unstabilized silver nanoparticles (μg/cm^3)			
	30 μg/cm^3	40 μg/cm^3	50 μg/cm^3	60 μg/cm^3	30 μg/cm^3	40 μg/cm^3	50 μg/cm^3	60 μg/cm^3
Escherichia coli XLIB	11.33 mm (±0.57)	15.33 mm (±0.57	20.4 mm (±0.55)	24.33 mm (±0.51)	10.33 mm (±0.51)	11.6 mm (±0.54)	17.6 mm (±0.57)	20.4 mm (±0.55)
Lysinibacillus fusiformis	10.67 mm (±0.54)	14.2 mm (±0.44)	21.33 mm (±0.51)	22.8 mm (±0.44)	10.67 mm (±0.57)	13.3 mm (±0.5)	18.33 mm (±0.55)	20.6 mm (±0.54)

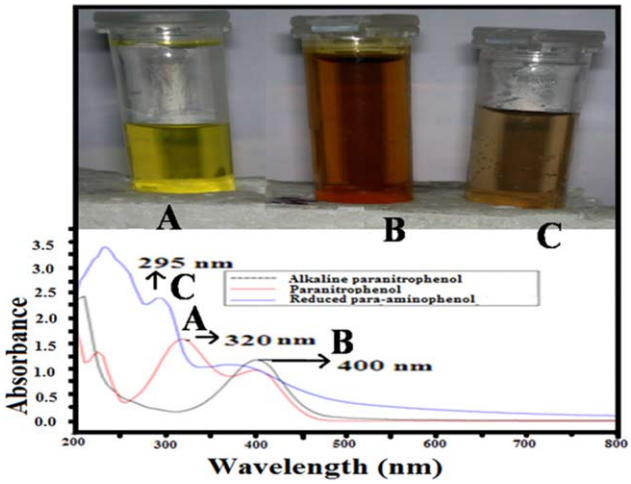

Figure 10. UV–visible absorption spectra of aqueous solutions of (A) pure 4-nitrophenol, (B) 4-nitrophenolate ion, (C) pure 4-aminophenol and Image of color (A). Pure para-nitrophenol, (B) alkaline para-nitrophenolate ion with silver nanosol and (C) pure para-aminophenol solution. [Color figure can be viewed in the online issue, which is available at wileyonlinelibrary.com.]

capping by polymeric network and corroborate the results of UV–Vis spectroscopy.

But, in the case of nonstabilized nanoparticles, the particles were bigger and more strongly aggregated [Figure 7(A,C)] than biopolymer stabilized nanoparticles as shown in Figure 7(B,D). The sizes of these aggregated assemblies were found to be 40–90 nm.

Antimicrobial Analysis

Antimicrobial activity of polymer stabilized and unstabilized silver nanoparticles which were synthesized by *Alkaliphilus oremlandii* strain ohILAs showed an inhibitory effect against both *Escherichia coli* XL1B strain (gram-negative) and *Lysinibacillus fusiformis* strain (gram-positive) (Figure 8). The polymer protected silver nanoparticles [Figure 8(A,B)] showed a better inhibitory effect than unprotected nanoparticles [Figure 8(C,D)]. A series of different concentrated solutions [30, 40, 50, and 60 μg/cm^3] of polymer protected silver nanoparticles and non protected silver nanoparticles were used to investigate the bactericidal activity against *E.coli* XL1B and *Lysinibacillus fusiformis*. These results revealed that the minimum inhibitory concentration of Ag nanoparticles against a gram-negative strain, *Escherichia coli* XL1B and a gram-positive strain, *Lysinibacillus fusiformis* were 50 and 60 μg/cm^3 [Figure 9(A,B)]. The 100% inhibitory effect on gram-negative strain was due to the positively charged AgNps which exhibited a greater affinity towards the negatively charged bacterial cells, resulting in the bactericidal activity.[25] But, in the case of gram-positive strain, the same inhibitory effect was observed with an increasing of concentration (60 μg/cm^3) of silver nanoparticles (Table II). Similar kind of observation was reported by Sondi et al, where 50–60 μg/cm^3 solution of silver nanoparticles caused 100% inhibition of bacterial growth.[42] The exhibition of better inhibitory effect on gram-negative strain than that on gram-positive strain was due to the presence of a thicker peptide cell wall in gram

positive bacteria, protecting inner parts of the cell from the penetration of silver ions in the cytoplasm.[43] Polyhydroxyalkanoates protected nanoparticles with an average size of 22 nm could easily penetrate into the bacterial cell and finally destroyed the cell. But, in the case of unprotected silver nanoparticles (63–93 nm), the inhibitory effect was found to be less efficient; this is due to the larger available surface area in smaller particles for interaction with the cell wall having the larger available surface area for interaction would and thereby provide more bactericidal effect compared to the larger particles.[44]

Application of Silver Nanoparticle for Functional Group Conversion

Catalytic Reduction of 4-Nitrophenol. The catalytic property of polymer stabilized silver nanoparticles was carried out by using an aromatic nitro compound as a substrate and sodium borohydride as a reducing agent. In Figure 10(A), the absorption peak at 320 nm indicated the presence of pure *p*-nitrophenol compound. With the addition of small volumes of alkali in the reaction mixture, the strong absorption peak at 320 nm was shifted to 400 nm; this was due to the formation of 4-nitrophenolate ion in alkaline condition [Figure 10(B)]. The peak at 400 nm remained unchanged even for a couple of days in the absence of any catalyst. When AgNps was added to the solution of phenolate ion in presence of sodium borohydride, the yellow color of *p*-nitrophenol was found to change and ultimately resulting in the discoloration of the solution.[14] The absorption peak of the colorless solution was observed at 295 nm; this was due to the formation of *p*-aminophenol [Figure 10(C)]. But, finally a clear absorption band at 390 nm was appeared due to the plasmonic resonance of silver nanoparticles. This reduction can be visualized by the disappearance of the 400-nm peak along with the appearance of a new peak at 295 nm. The peak due to 4-aminophenol appeared after 7 min of addition of catalyst particles in the reaction mixture. Similar results were also observed by Gangula et al.[28] The reduction of aromatic functional group by the protected silver nanoparticles was also reported elsewhere.[43]

CONCLUSIONS

In summary, silver nanoparticles with a lower range of particles size (22–43 nm) was synthesized by the reduction of silver nitrate salt with the microbial strain, *Alkaliphilus oremlandii* strain ohILAs at an optimized pH 10. The biopolymer, polyhydroxyalkanoates was used as a capping and stabilizing agent to minimize the agglomeration of silver nanoparticles. The antimicrobial activity test showed that the degree of inhibition of the microbial growth increased with an increase in silver content and it was found to be more efficient in the presence of the polymer protected nanosilver. Again, the catalytic activity of the stabilized nanoparticles was kinetically more effective than non stabilized silver nanoparticles to reduce the aromatic nitro group. It may be due to their small surface area as well as their agglomeration tendency from the solution. Therefore, the biopolymer protected silver nanoparticles may find industrial application as an effective reducing agent and also for biomedical application.

ACKNOWLEDGMENTS

The authors gratefully acknowledge Technical Education Quality Improvement Programme (TEQIP), Government of India and CSIR grant-in-aid [No.02 (0008)/11/EMR-II], Government of India for their financial support in this experimental work.

REFERENCES

1. Pickett, N. L.; Brien, P. O. *Chem. Rec.* **2001**, *1*, 467.
2. Henglein, A. *Chem. Rev.* **1989**, *89*, 1861.
3. Riehemann, K.; Schneider, S. W.; Luger, T. A.; Godin, B.; Ferrari, M.; Fuchs, H. *Angew. Chem. Int. Ed Engl.* **2009**, *48*, 872.
4. Khlebtsov, B. N.; Panfilova, E. V.; Terentyuk, G. S.; Maksimova, I. L.; Ivanov, A. V.; Khlebtsov, N. G. *Langmuir* **2012**, *28*, 8894.
5. Toshima, N. *Supramol. Sci.* **1998**, *5*, 395.
6. Agrawal, A.; Paul, G. T. *Environ. Sci. Technol.* **1996**, *30*, 153.
7. Fonseca, S. G.; Umpierre, P. A.; Fichtner, P. F. P.; Teixeira, R. S.; Dupont, J. *Chem. Eur. J.* **2003**, *9*, 3263.
8. Klingelhöfer, S.; Heitz, W.; Greiner, A.; Oestreich, S.; Förster, S.; Antonietti, M. *J. Am. Chem. Soc.* **1997**, *119*, 10116.
9. Kim, S. W.; Son, S. U.; Lee, S. S.; Hyeon, T.; Chung, Y. K. *Chem. Commun.* **2001**, 2212.
10. Kim, S. W.; Kim, M.; Lee, W. Y.; Hyeon, T. *J. Am. Chem. Soc.* **2002**, *124*, 7642.
11. Toshima, N.; Takahashi, T.; Hirai, H. *J. Macromol. Sci. Chem. A* **1988**, *25*, 669.
12. Toshima, N.; Takahashi, T. *Bull. Chem. Soc. Jpn.* **1992**, *65*, 400.
13. Satyavani, K.; Gurudeeban, S.; Ramanathan, T.; Balasubramanian, T. *J. Nanobiotechnol.* **2011**, *9*, 43.
14. Pradhan, N.; Pal, A.; Pal, T. *Colloids Surf. A: Physicochem. Eng. Aspects* **2002**, *196*, 247.
15. Parikh, D. V.; Fink, T.; Rajasekharan, K.; Sachinvala, N. D.; Sawhney, A. P. S.; Calamari, T. A.; Parikh, A. D. *Text. Res. J.* **2005**, *75*, 134.
16. Chatterjee, D. K.; Fong, L. S.; Zhang, Y. *Adv. Drug Deliv. Rev.* **2008**, *60*,1 627.
17. Patel, A.; Prajapati, P.; Boghra, R. *Asian J. Pharmaceut. Sci. Clin. Res.* **2011**, *1*, 40.
18. Kowshik, M.; Ashtaputre, S.; Kharrazi, S.; Vogel, W.; Urban, J.; Kulkarni, S. K.; Paknikar, K. M. *Nanotechnology* **2003**, *14*, 95.
19. Vaidyanathan, P.; Kalishwaralal, K.; Gopalram, S.; Gurunathan, S. *Biotechnol. Adv.* **2009**, *27*, 924.
20. Slawson, R. M.; VanDyke, R. M.; Lee, H.; Trevor, J. T. *Plasmid* **1992**, *27*, 72.
21. Irwin, P.; Martin, J.; Nguyen, L. H.; He, Y.; Gehring, A.; Chen, C. Y. *J. Nanobiotechnol.* **2010**, *8*, 34.
22. Sondi, I.; Sondi, B. S. *J Colloid Interface Sci.* **2004**, *275*, 177.
23. Nanda, A.; Saravanan, M. *Nanomed. Nanotechnol. Biol. Med.* **2009**, *5*, 452.
24. Kim, K. J.; Sung, W. S.; Moon, S. K.; Choi, J. S.; Kim, J. G.; Lee, D. G. *J. Microbiol. Biotechnol.* **2008**, *18*, 1482.

25. Elechiguerra, J. L.; Burt, J. L.; Morones, J. R.; Camacho, A. B.; Gao, X.; Lara, H. H.; Yacaman, M. J. *J. Nanobiotechnol.* **2005**, *3*, 6.

26. Lakshmipathy, M.; Nanda, A. *Int. J. Chem. Tech. Res.* **2013**, *5*, 1162.

27. Pozun, D. Z.; Rodenbusch, E. S.; Keller, E.; Tran, K.; Tang, W.; Stevenson, J. K.; Henkelman, G. *J. Phys. Chem. C* **2013**, *117*, 7598.

28. Gangula, A.; Podila, R.; Ramakrishna, M.; Karanam, L.; Janardhana, C.; Rao, N. A. *Langmuir* **2011**, *27*, 15268.

29. Rawte, T.; Mavinkurve, S. *Indian J. Expt. Biol.* **2002**, *40*, 924.

30. Pramanik, N.; Mukherjee, K.; Nandy, A.; Mukherjee, S.; Kundu, P. P. *J. Appl. Polym. Sci.* **2014**, *131*, 41080.

31. Das, L. V.; Thomas, R.; Varghese, T. R.; Soniya, E. V.; Mathew, J.; Radhakrishnan, K. E. *3 Biotech* **2014**, *4*, 121.

32. Natarajan, K.; Selvaraj, S.; Murty, V. R. *Dig. J. Nanomater. Biostruct.* **2010**, *5*, 135.

33. Venkataraman, V. D.; Umamaheshwaran, P. S.; Guhan, K.; Nanthini, R. A.; Krithiga, B.; Hasika Jaithoon, N. M.; Gurunathan, S. *Colloids Surf. B: Biointerfaces* **2011**, *86*, 353.

34. Phukon, P.; Saikia, J. P.; Konwar, B. K. *Colloids Surf. B: Biointerfaces* **2011**, *86*, 314.

35. Xia, Y.; Halas, N. *J. MRS Bull.* **2005**, *30*, 338.

36. Knox, J. K. W.; Cullen, U. *Biochem. J.* **1967**,*103*, 192.

37. Durán, N.; Marcato, P. D.; Alves, O. L.; Souza, G. I.; Esposito, E. *JoN* **2005**, *3*, 8.

38. Senapati, S.; Ahmad, A.; Khan, M. I.; Sastry, M.; Kumar, R. *Small* **2005**, *1*, 517.

39. Gardea, J. L.; Torresdey, E.; Gomez, J. R.; Videa, J. G.; Parsons, H.; Troiani, M.; Yacaman, J. *Langmuir* **2003**, *19*, 1357.

40. Kannan, N.; Mukunthan, K. S.; Balaji, S.; Don, G. *Colloids Surf. B: Biointerfaces* **2011**, *86*, 378.

41. Sondi, I. I.; Salopek, S. B. *J. Colloid Interface Sci.* **2004**, *275*, 177.

42. Rai, M.; Yadav, A.; Gade, A. *Biotechnol. Adv.* **2009**, *27*, 76.

43. Kundu, S.; Mandal, M.; Ghosh, S. K.; Pal, T. *J. Colloid Interface Sci.* **2004**, *272*, 134.

44. Lok, C. M.; Ho, C. M.; Chen, R. Q.; He, Y.; Yu, W. Y.; Sun, H.; Tam, P. K.; Chiu, J. F.; Che, C. M. *J. Proteome Res.* **2006**, *5*, 916.